COMMUNICATION

A Polyferroplatinyne Precursor for the Rapid Fabrication of $L1_0$-FePt-type Bit Patterned Media by Nanoimprint Lithography

Qingchen Dong, Guijun Li, Cheuk-Lam Ho, Mahtab Faisal, Chi-Wah Leung, Philip Wing-Tat Pong, Kun Liu, Ben-Zhong Tang, Ian Manners,* and Wai-Yeung Wong**

As the magnitude of information created and stored grows exponentially, a new type of magnetic material with ultrahigh density for data recording is urgently needed in a modern society. $L1_0$ phase (or face-centered tetragonal, fct, phase) FePt alloy nanoparticles (NPs) have been studied extensively in the last decade, because of their interesting redox, catalytic, and magnetic properties.[1,2] The use of $L1_0$-ordered FePt NPs as the candidate for the ultrahigh-density magnetic data storage media is a consequence of its extraordinarily large uniaxial magnetocrystalline anisotropy (which can reach up to $K_u \approx 7 \times 10^6$ J m^{-3}) in the bulk phase and high chemical stability. This has inspired scientists to explore different methods to generate $L1_0$-ordered FePt NPs with controllable size and high coercivity (a parameter indicative of magnetocrystalline anisotropy) which are closely related to the size and purity of NPs.[3–5] The most common approach adopted to synthesize the $L1_0$ phase FePt NPs involves refluxing a mixture of individual Fe- and Pt-containing compounds in a high-boiling organic solvent, and the resulting A_1-ordered (or face-centered cubic, fcc, phase) FePt NPs are then thermally annealed to give the desirable $L1_0$ phase. Inevitably, some defects such as sintering, agglomeration, broad size distribution, etc, will be concomitant with this method.[6,7] The reason for these problems could be attributed to the fact that the elements Fe and Pt are originally in separate compounds which have different onset decomposition temperatures. Hence, some organometallic complexes containing both Fe and Pt atoms for use as a single source precursor were synthesized and applied to generate the $L1_0$ phase FePt NPs by the one-step decomposition.[8,9] However, direct and rapid patterning of the target FePt NPs is also a substantial challenge for many practical applications, which demand precise reading out and direct-writing onto the NPs. In particular, bit patterned media (BPM) made with FePt NPs are promising candidates for the next generation of magnetic recording systems. Even though some recent efforts on the fabrication of monodisperse FePt NP thin films have been made by self-assembly processes, they are not suitable for the generation of ordered $L1_0$ phase FePt nanopatterned arrays over large areas and on a large scale.[10,11]

In the last decade, owing to the key advantage of the film-forming and self-assembly properties of metallopolymers, patterned metal NPs over large areas can be achieved on various substrates by pyrolysis or photolysis of the patterned metallopolymers, and such work is important for many applications based on metal nanostructures.[12,13] We have recently reported a convenient one-pot method to directly synthesize $L1_0$ FePt alloy NPs through the pyrolysis of a metallopolymer containing both Fe and Pt atoms.[14] Although this polymer had poor solubility, we could still exploit it in the formation of pure chemically ordered FePt NPs and in the fabrication of arrays of ferromagnetic FePt NP micropatterns because of its high feasibility and utility in patterning. Traditional methods such as UV photolithography only provide sub-micrometer resolution and electron-beam lithography is not suitable for the fabrication of ordered nanostructured arrays of magnetic NPs over large areas owing to the restrictions of high cost, complicated procedures, and high demand of the materials.[15,16] Nanoimprint lithography (NIL) is a new and powerful technology for high-throughput patterning with high resolution and at very low cost.[15] It has been used to imprint different kinds of polymers, allowing its wide application in electronics, photonics, information storage and biotechnology.[15,17] Since NIL offers sub-5 nm patterning resolution over very large areas, it is indeed desirable for fabricating BPM. Unlike traditional lithographic approaches, which achieve

Q. C. Dong, Dr. C.-L. Ho, Prof. W.-Y. Wong
Institute of Molecular Functional Materials
Department of Chemistry and Institute of Advanced Materials
Hong Kong Baptist University
Waterloo Road, Hong Kong, P. R. China
E-mail: rwywong@hkbu.edu.hk
G. J. Li, Prof. P. W.-T. Pong
Department of Electrical and Electronic Engineering
The University of Hong Kong
Pokfulam Road, Hong Kong, P. R. China
E-mail: ppong@eee.hku.hk
Dr. M. Faisal, Prof. B. Z. Tang
Department of Chemistry
The Hong Kong University of Science and Technology
Clearwater Bay, Hong Kong, P. R. China
Prof. C. W. Leung
Department of Applied Physics
Hong Kong Polytechnic University
Hung Hom, Hong Kong, P. R. China
Dr. K. Liu
Department of Chemistry
University of Toronto
Toronto, M5S 3H6, Canada
Prof. I. Manners
School of Chemistry
University of Bristol
Bristol, BS8 1TS, UK
E-mail: Ian.Manners@bristol.ac.uk

DOI: 10.1002/adma.201104171

pattern definition through the use of photons or electrons to modify the chemical and physical properties of the resist, NIL relies on direct mechanical molding of the resist material and can therefore achieve resolution beyond the limitations set by light diffraction or beam scattering that are often encountered in the conventional techniques. Although the nanoimprinting technique has been recently used with FePt continuous thin films, multiple processing steps are necessary for preparing the nanosized bits.[18] It has been difficult to create BPM with FePt NPs by NIL because the mechanical rigidity of NPs does not allow them to transfer the negative pattern of the mask directly. In this work, a new polymeric material has been developed which combines the merits of both FePt NPs and nanoimprint lithography, thereby providing a single-step fabrication of BPM at a relatively low cost. We report here a new bimetallic polymer containing both Fe and Pt atoms with excellent solubility in many organic solvents, and the nanofabrication of line array and dot array patterns of $L1_0$ phase hard magnetic FePt NPs by the soft NIL technique using it as a practical single-source precursor. To our knowledge, this is the first literature report to adopt NIL to achieve the high-throughput patterning of $L1_0$ phase FePt NPs with nanoscopic features.

Figure 1a shows the chemical structure of the target metallopolymer **P**. Synthesis of **P** is described in the Supporting Information. Through direct pyrolysis of **P**, the $L1_0$ phase FePt alloy NPs can be generated directly without the need of any post-annealing step. Figure 1b shows a transmission electron microscopy (TEM) image of FePt NPs surrounded by a carbonaceous matrix which can prevent the aggregation of the FePt NPs. Figure 1c shows a high-resolution TEM image of a single FePt NP with well-faceted spherical morphology, indicating that the resulting FePt NPs are of high crystallinity. The lattice fringes of the FePt NPs measured from the high-resolution TEM image are 0.377, 0.224 and 0.278 nm respectively, which are in good agreement with the literature values of 0.385 nm for the (100) planes, 0.219 nm for the (111) planes and 0.272 nm for the (110) planes of chemically ordered fct structure of FePt alloy NPs.[19] The particle size and size distribution of the resulting FePt NPs were also investigated from the analysis of the TEM image. The particles have an effective average size of 4.6 ± 1.2 nm with a reasonably narrow standard deviation as depicted in Figure 1d. The results of energy-dispersive X-ray (EDX) elemental analysis show the composition of the resultant FePt alloy NPs to be approximately 50:50 for the atomic ratio of Fe to Pt, which is consistent with the expected stoichiometry from the polymer precursor **P**.

The composition and structure of the as-formed FePt NPs were also studied by powder X-ray diffraction (PXRD). Figure 1e shows a PXRD plot of the FePt NPs synthesized by the pyrolysis of **P** at 800 °C for 1 h under Ar atmosphere. The (001) and (110) peaks represent the characteristic peaks of $L1_0$-structured FePt

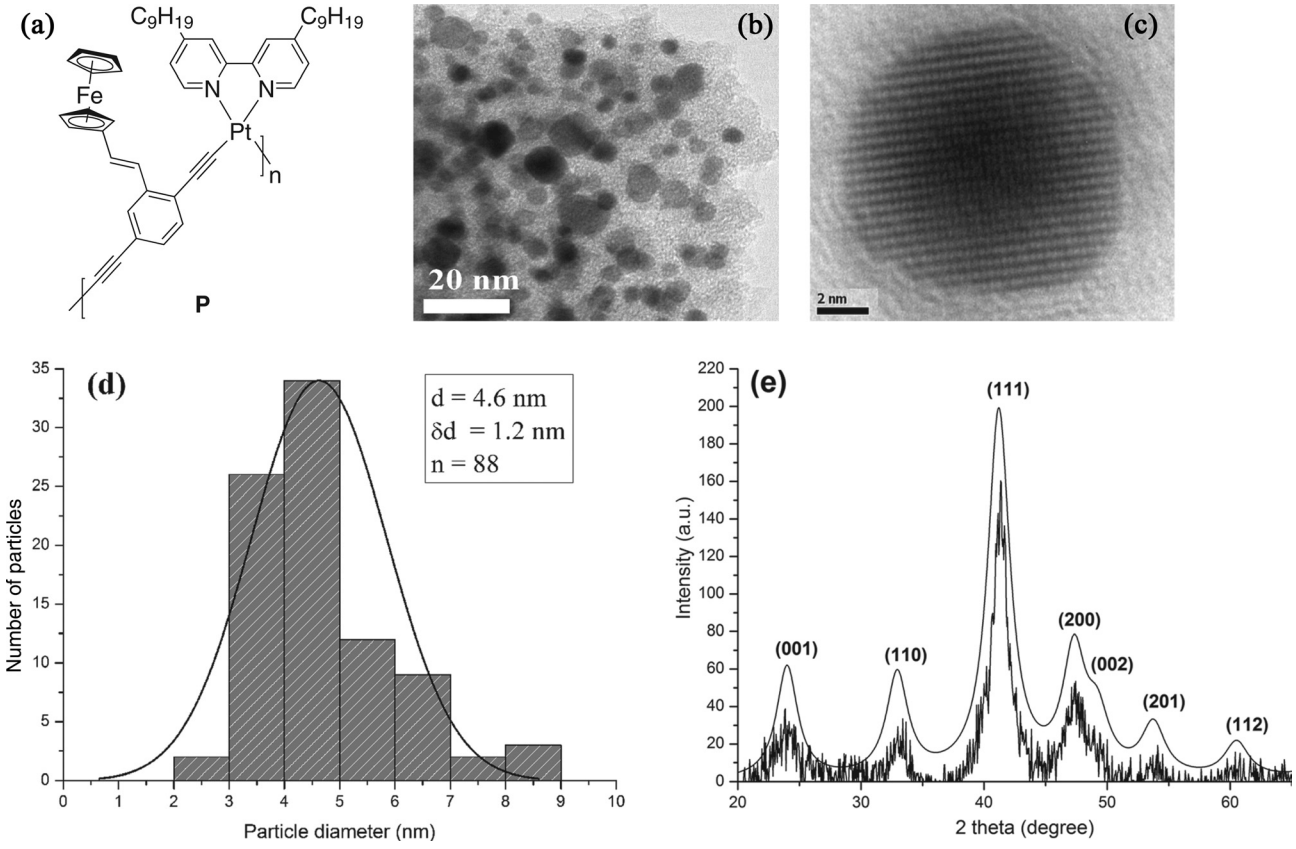

Figure 1. (a) Chemical structure of metallopolymer **P**. (b) TEM characterization of FePt NPs synthesized through direct pyrolysis of **P** at 800 °C for 1 h under Ar. (c) A high resolution TEM image of a single FePt NP. (d) A particle-size histogram measured from the TEM image in (b). (e) Powder X-ray Rietveld plot of the FePt NPs synthesized at 800 °C for 1 h under Ar.

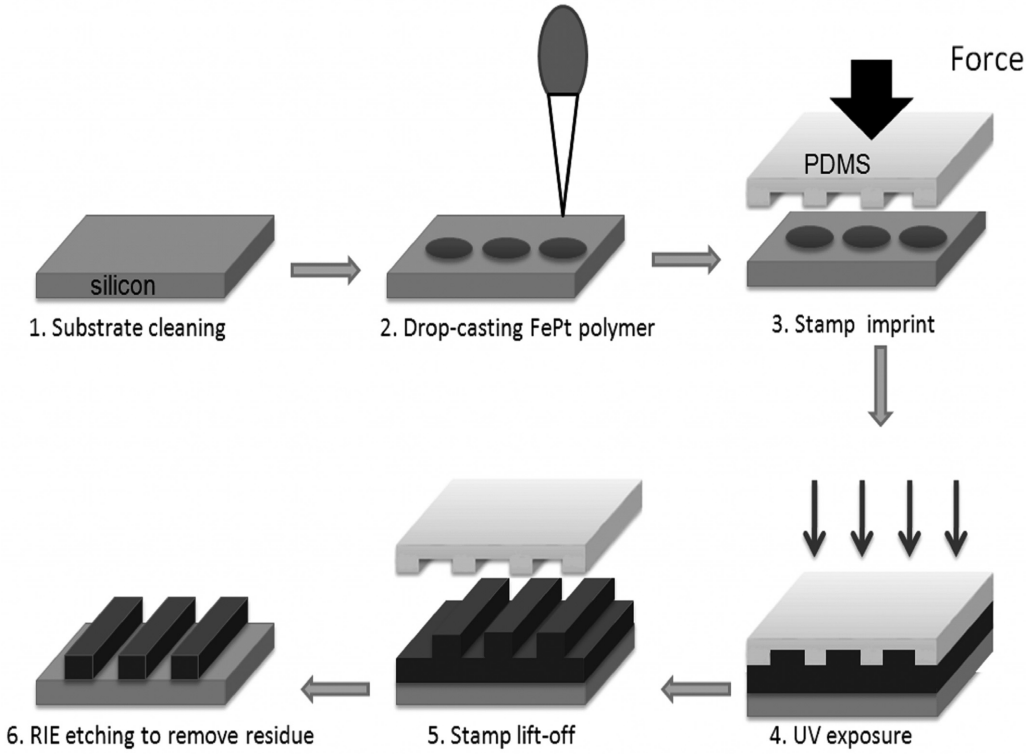

Figure 2. Schematic illustration of the fabrication of large-area nanostructures from the FePt-based metallopolymer **P** by nanoimprinting. (1) A silicon substrate is cleaned with acetone and deionized water together with sonication. (2) A polymer **P** is drop-cast onto the silicon substrate with a dropper. (3) The PDMS stamp is pressed onto the sample with a uniform force. (4) The whole sample and the stamp are irradiated with UV light to induce cross-linking. (5) The FePt-containing bimetallic polymer undergoes cross-linking and solidifies. The stamp is then lifted off. (6) The residue is removed by RIE etching.

NPs, which are evident unequivocally in the PXRD spectrum. This further confirms that the structure of FePt NPs is chemically ordered fct. The fitted smooth line stands for the curve generated from the Rietveld refinement, which matches that obtained by experiment. The mean domain size evaluated by the Rietveld analysis is approximately 5 nm which is consistent with that measured from the TEM image, indicating that the as-synthesized $L1_0$ FePt NPs are composed of nanosized crystalline domains. The ordering parameter S was determined to be 1.004, which indicates the high chemically ordered phase present in this sample ($S = 1$ means the fully ordered phase). Hence, the observed peak broadening in the PXRD spectrum can be attributed to the small size of NPs instead of structural disorder.[8]

Figure 2 depicts the procedure of nanoimprint molding the bimetallic polymer **P**. Firstly, a silicon substrate was rinsed in acetone followed by deionized water coupled with sonication. Then, a saturated solution of **P** in chloroform was drop-cast onto the substrate. A stamp made of polydimethylsiloxane (PDMS) was then used to imprint patterns onto the silicon substrate with a constant and uniform force. The PDMS nanoimprint stamps used in this study include a line array nanopattern with periodicity (feature size) of 740 nm (350 nm) and a dot array nanopattern with periodicity (feature size) of 500 nm (250 nm). The soft PDMS molds were cast from original masks as described previously.[20,21] Exposing the sample to ultraviolet radiation (25 mW cm^{-2}, 391 nm) for 5 min presumably cross-linked the metallopolymer and transformed the mixed-metal FePt-containing polymer with low molecular weight into one with higher molecular weight. The chloroform solvent was evaporated in this step and left the mixed-metal polymer in the solid phase. Then, the PDMS mask was lifted from the substrate surface and a negative copy of the pattern was replicated to the FePt-based polymer on the sample surface. Next, the sample was dry etched with reactive ion etching (RIE) to remove any residue in the trenches. Finally, the sample was annealed at 800 °C under argon for 1 h to transform the polymer into FePt alloy NPs.

For making BPM with a continuous FePt thin film by NIL, the photoresist must first be spun and patterned using NIL. Then, either the FePt thin film is etched away (subtractive process) or the FePt thin film is deposited and lifted off (additive process). This is in contrast to the single-step fabrication process with the FePt-based metallopolymer **P**. This process takes advantage of the solubility of **P** and imprints the polymer directly in the liquid phase, thereby eliminating the prior step of spinning and patterning the photoresist and the subsequent step of etching/lift-off of FePt thin film.

The metallopolymer **P** was patterned at the nanoscale with high accuracy by the imprinting approach. **Figure 3**a shows the scanning electron microscope (SEM) image of the imprinted polymer **P** with a nanoscale line array pattern. Measurements

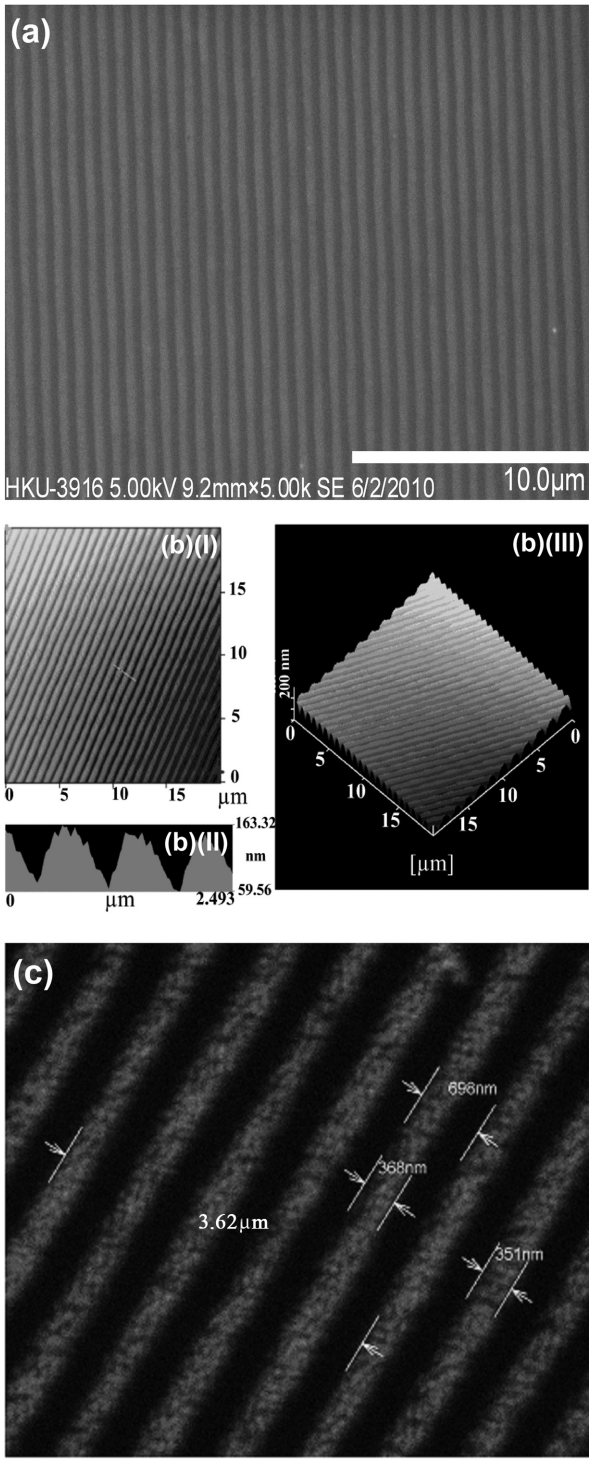

Figure 3. (a) SEM image of the nanoimprinted line array pattern of **P**. The pattern periodicity and feature size were measured to be approximately 740 nm and 350 nm, respectively. (b) (I) Topographic AFM image of the nanoimprinted line array pattern of **P**. The pattern periodicity and feature size were measured to be approximately 740 nm and 350 nm, respectively. (II) Cross-section analysis showing the feature height to be around 100 nm. (III) 3D AFM image showing the topography of the nanoimprinted line array pattern. (c) SEM image of the nanoimprinted line array pattern of FePt NPs after pyrolysis. The pattern periodicity and feature size were measured to be approximately 740 nm and 350 nm, respectively.

of the line array periodicities and widths show high conformity of the final pattern to the imprint mold. From Figure 3b(I), the topography of the imprinted pattern was characterized by atomic force microscopy (AFM). From the cross-section analysis displayed in Figure 3b(II), the height of this line array pattern on the substrate was measured to be approximately 100 nm. This is close to the depth of the line array pattern on the stamp. As depicted from Figure 3b(III) which shows the three-dimensional (3D) topographical image of the line array pattern on the sample substrate, the pattern and structure of the imprinted bimetallic FePt-containing polymer **P** can be controlled and defined by the stamp.

The sample with track periodicity of 740 nm and feature size of 350 nm was then annealed at 800 °C for 1 h under argon in the pyrolysis experiment. As shown in Figure 3c, the imprinted line array pattern was preserved after pyrolysis. The feature size and the pattern periodicity were not altered by the thermolysis. After the successful imprinting and pyrolysis of **P** with a feature size of 350 nm, a PDMS stamp with a hole array pattern of hole diameter of 250 nm and periodicity of 500 nm was used to imprint the polymer **P**; this served as a prototype for the simple and rapid fabrication of BPM on a substrate. **Figure 4**a illustrates the scanning electron microscopy (SEM) image of the imprinted dot array of **P**. From the image, the diameter of the imprinted dots was measured to be around 250 nm with periodicity of around 500 nm. The sample was then pyrolyzed at 800 °C for 1 h under argon. After pyrolysis, a DC magnetic field of 1 Tesla (or 10^4 Oe) was applied in the out-of-plane direction to magnetize the sample in a preferred direction.

The topography of the pyrolyzed dot array NPs was characterized by AFM (see Figure 4b). The height of the dot array was measured to be around 5 nm to 8 nm. This was relatively small compared with the depth of the original PDMS mold (80 nm) which could be attributed to the collapse of the material after pyrolysis at high temperature. Nevertheless, the effect of imprinting on pattern formation was clearly observed. The bulk magnetic property of the sample after pyrolysis was characterized by vibrating sample magnetometer (VSM). The hysteresis loop measured at room temperature is shown in Figure 4c. The coercivity of the patterned sample was measured to be around 1.4 T at room temperature which is sufficiently large for high-density magnetic data storage applications today.[21–23] Thus, these physically separated magnetic dots, each consisting of $L1_0$ phase FePt NPs, can be written by an external field to record information which forms the basis for BPM to write and read data.

To further demonstrate this concept, the well-patterned metallopolymer dot array was allowed to be field-annealed in the –Z direction with an external magnetic field of 1 T for 1 h at 800 °C to form dot array of FePt NPs with parallel magnetic direction, and then the magnetic direction of the resultant ferromagnetic FePt NPs dot array was switched to the +Z direction by applying an external magnetic field of 1.8 T at room temperature. We can observe the surface topography and the magnetization of the above ferromagnetic FePt NPs dot array in different magnetic directions (**Figure 5**).

3D AFM images of the samples are shown in Figure 5a and 5c (Inset: top view). The dot array structural patterns can be clearly observed with the same pre-defined periodicity on

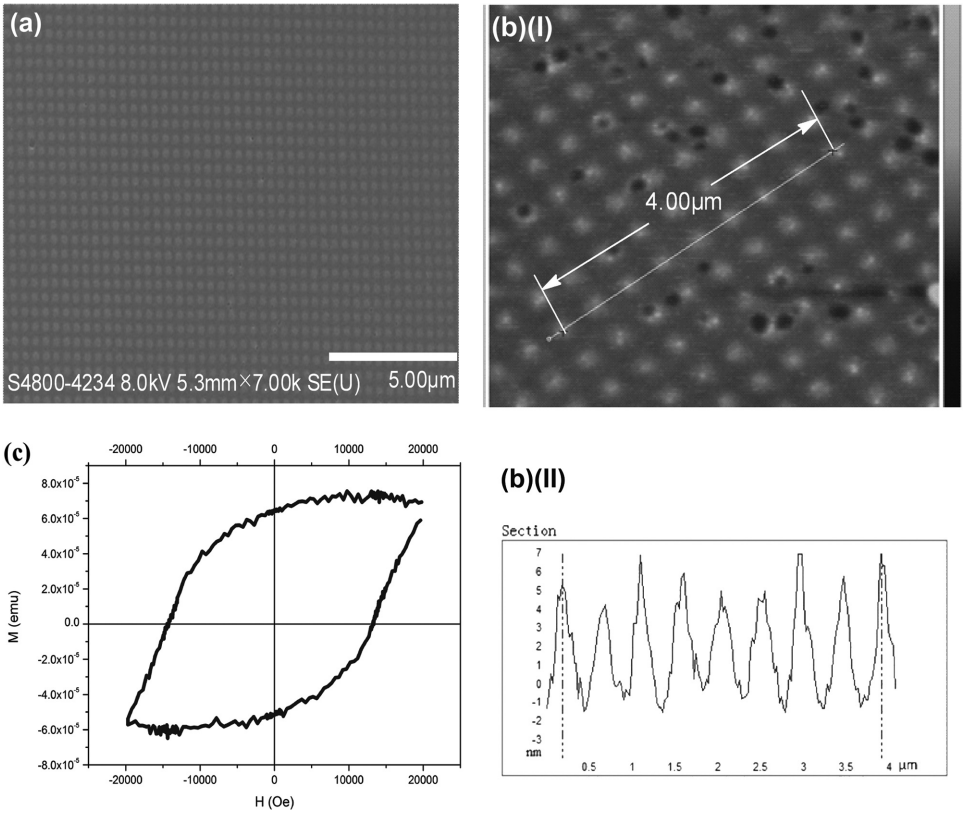

Figure 4. (a) SEM image of the nanoimprinted dot array pattern of **P**. The pattern periodicity and the feature size are approximately 500 nm and 250 nm, respectively. (b) (I) AFM image of nanoimprinted dot array FePt NPs after pyrolysis of **P**. The pattern periodicity and the feature size were measured to be approximately 500 nm and 250 nm, respectively. (II) Cross-section analysis of the measured distance as indicated in (b)(I). (c) Hysteresis loop measurement by VSM at room temperature in the out-of-plane direction of the nanoimprinted dot array pattern of FePt NPs after pyrolysis. The coercivity was measured to be 1.4 T at room temperature.

both samples. The corresponding 3D magnetic force microscopy (MFM) images (see Figure 5b and 5d; inset: top view) were taken in the interleave mode. In the interleave mode, the cantilever was first scanned over the surface to acquire the topographical information; in the second pass, the cantilever was lifted up by 100 nm so that the topographical information can be avoided and only the magnetic signal was acquired. As such, only magnetization information (without surface topography) was acquired in the above MFM images. In Figure 5b, we can see a dot array nanopattern of magnetization with the same periodicity as the dot array pattern in the corresponding AFM image (Figure 5a) which indicates that this dot array nanopattern is magnetic. Figure 5d shows the MFM image of the sample in which the magnetic direction was reversed. Similarly, a dot array nanopattern of magnetization with the same periodicity as the dot array pattern in the topography scan can be seen. However, the contrast in this MFM image (Figure 5d) is opposite to that of the sample field-annealed in the –Z direction (Figure 5b). The dot array pattern of magnetization is dark in Figure 5d whereas it is bright in Figure 5b. This indicates that the magnetization directions of these two dot array nanopatterns are opposite to each other. Therefore, the magnetization direction can be manipulated to point "up" or "down" by applying an external magnetic field in alternate magnetic directions, which underpins the basis of magnetic data recording. Our prototype BPM here provides an areal density of 2.58 Gb in^{-2}. Solid-mold nanoimprinting with a pitch of 25 nm and sub-15 nm feature sizes has been previously demonstrated[24,25] which could provide an areal density of 1 Tb in^{-2}. Such an areal density is already in par with the latest hard-disk drives reported in 2011 whose areal densities are around 0.5 to 1 Tb in^{-2}.[26] State-of-the-art nanoimprint lithography can achieve sub-15 nm pitch size and sub-10 nm features,[27] which is equivalent to an areal density of 2.8 Tb in^{-2}. Patterning pitch down to 12 nm (equivalent to 4.3 Tb in^{-2}) was already realized with good uniformity in the market.[28] As such, provided that a stamp with the corresponding pattern is taken, our FePt-based metallopolymer in conjunction with NIL can potentially offer an alternative route for achieving a BPM with a storage density beyond 1 Tb in^{-2} into a regime which the existing technology cannot reach,[29] without resorting to the use of extremely sophisticated fabrication techniques (such as electron-beam or X-ray lithography) to pattern such features.

In conclusion, a new polyferroplatinyne polymer containing both Fe and Pt atoms with useful solution processability in organic solvents was employed as a single-source binary metal

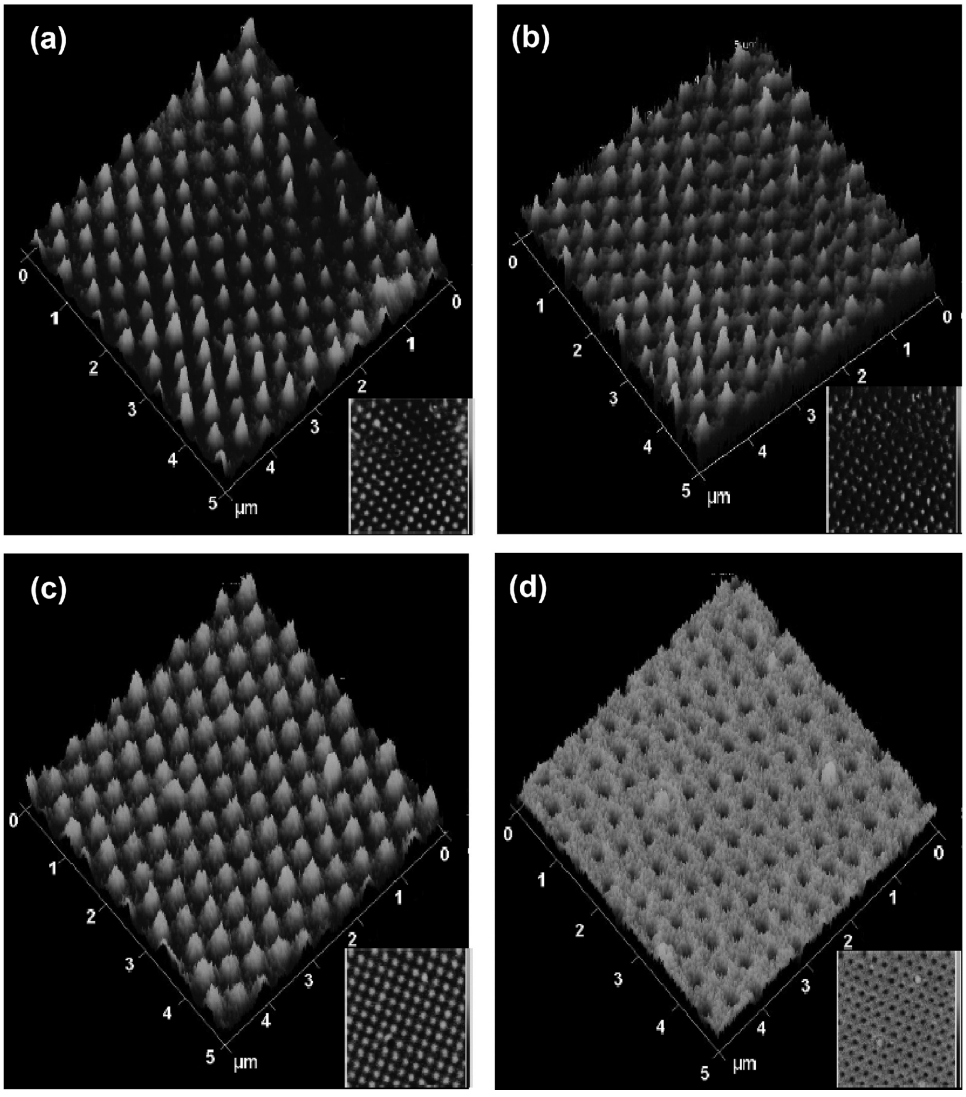

Figure 5. (a) AFM image and (b) MFM image of the nanoimprinted dot array pattern of FePt NPs field-annealed in the –Z direction with a periodicity of approximately 500 nm and the feature size of around 250 nm. (c) AFM image and (d) MFM image of the nanoimprinted dot array pattern of FePt NPs field-annealed in the +Z magnetic direction with the same periodicity and feature size.

alloy NP precursor, from which $L1_0$ phase FePt NPs of reasonably narrow size distribution (average size of 4.6 nm) were produced. We also report a novel single-step approach to generate nanopatterned arrays of $L1_0$ phase FePt NPs as a BPM prototype with high throughput by NIL. The nanopatterned arrays of FePt NPs possess a room-temperature coercivity as large as 1.4 T (i.e. 14 kOe) which is comparable to those values of the magnetic recording media currently in use. The MFM images of the nanodot patterns also clearly demonstrate that the magnetization directions of the patterned $L1_0$ phase FePt NPs can be adjusted to show "up" or "down", and this proof-of-principle magnetic recording experiment can be utilized as the new platform for BPM and next generation of nanoscale high-density magnetic data storage devices where convenient and rapid nanopatterning of magnetic NPs at low cost is highly essential. The current approach can simplify the manufacturing procedure of BPM without the need for photoresist, etching, or lift-off. Moreover, since the new material has excellent solubility in organic solvents, soft stamps can be employed to confer conformal contact which is favourable for long-range order using only a minimal pressure. Hence, the defect rate of magnetic bits can be suppressed, the overall product yield can be improved, and the throughput can be enhanced. Additionally, this technique is generic in nature, and can be readily adopted for the rapid nanopatterning of complex NPs with designed features on many surfaces, such kind of patterns are of high demand in areas such as photovoltaics[30] and biochemical sensing applications.[31] In the future, we will focus on the creation of patterns of ferromagnetic FePt alloy NPs at further reduced dimensions down to tens of nanometers in order to achieve an areal density of over 1 Tb in^{-2}. Such nanotransfer printing method is directly applicable to the fabrication of 3D nanopatterned arrays that are scalable to arbitrarily large areas and are compatible with manufacturing.

Supporting Information

Supporting Information is available from the Wiley Online Library or from the author.

Acknowledgements

Q.C. Dong and G. J. Li contributed equally to this work. We acknowledge the financial support from the Hong Kong Research Grants Council (HKBU202508 and HKUST2/CRF/10), Areas of Excellence Scheme from the University Grants Committee (AoE/P-03/08) and a FRG grant from Hong Kong Baptist University of Hong Kong SAR (FRG2/09-10/091).

Received: October 30, 2011
Published online: January 31, 2012

[1] S. Sun, *Adv. Mater.* **2006**, *18*, 393.
[2] N. A. Frey, S. Peng, K. Cheng, S. Sun, *Chem. Soc. Rev.* **2009**, *38*, 2532.
[3] S. Sun, C. B. Murray, D. Weller, L. Folks, A. Moser, *Science* **2000**, *27*, 1989.
[4] a) D. Weller, A. Moser, *IEEE Trans. Magn.* **1999**, *35*, 4423; b) J. P. Wang, *Proceedings of the IEEE* **2008**, *96*, 1847.
[5] A. Moser, *J. Phys. D: Appl. Phys.* **2002**, *35*, R157.
[6] T. Thomson, S. L. Lee, M. F. Toney, C. D. Dewhurst, F. Y. Ogrin, C. J. Oates, S. Sun, *Phys. Rev. B* **2005**, *72*, 064441-1.
[7] H. L. Nguyen, L. E. M. Howard, G. W. Stinton, S. R. Giblin, B. K. Tanner, I. Terry, A. K. Hughes, I. M. Ross, A. Serres, J. S. O. Evans, *Chem. Mater.* **2006**, *18*, 6414.
[8] A. Capobianchi, M. Colapietro, D. Fiorani, S. Foglia, P. Imperatori, S. Laureti, E. Palange, *Chem. Mater.* **2009**, *21*, 2007.
[9] M. S. Wellons, W. H. Morris, Z. Gai, J. Shen, J. Bentley, J. E. Wittig, C. M. Lukehart, *Chem. Mater.* **2007**, *19*, 2483.
[10] J. Kim, C. Rong, J. P. Liu, S. Sun, *Adv. Mater.* **2009**, *21*, 906.
[11] M. Suda, Y. Einaga, *Angew. Chem. Int. Ed.* **2009**, *48*, 1754.
[12] a) B. C. Englert, S. Scholz, P. J. Leech, M. Srinivasarao, U. H. F. Bunz, *Chem. Eur. J.* **2005**, *11*, 995; b) G. R. Whittell, M. D. Hager, U. S. Schubert, I. Manners, *Nat. Mater.* **2011**, *10*, 176; c) W.-Y. Wong, *Dalton Trans.* **2007**, *40*, 4495.
[13] a) T. Ruotsalainen, J. Turku, P. Heikkilä, J. Ruokolainen, A. Nykänen, T. Laitinen, M. Torkkeli, R. Serimaa, G. Brinke, A. Harlin, O. Ikkala, *Adv. Mater.* **2005**, *17*, 1048; b) C. K. W. Jim, A. Qin, F. Mahtab, J. W. Y. Lam, B. Z. Tang, *Chem. Asian J.* **2011**, *6*, 2753; c) S. B. Clendenning, S. Aouba, M. S. Rayat, D. Grozea, J. B. Sorge, P. M. Brodersen, R. N. S. Sodhi, Z. H. Lu, C. M. Yip, M. R. Freeman, H. E. Ruda, I. Manners, *Adv. Mater.* **2004**, *16*, 215.
[14] K. Liu, C. L. Ho, S. Aouba, Y. Q. Zhao, Z. H. Lu, S. Petrov, N. Coombs, P. Dube, H. E. Ruda, W. Y. Wong, I. Manners, *Angew. Chem. Int. Ed.* **2008**, *47*, 1255.
[15] L. Guo, *Adv. Mater.* **2007**, *19*, 495.
[16] Q. Guo, X. Teng, H. Yang, *Adv. Mater.* **2004**, *15*, 1337.
[17] K. Liu, S. Fournier-Bidoz, G. A. Ozin, I. Manners, *Chem. Mater.* **2009**, *21*, 1781.
[18] T. Bublat, D. Goll, *Nanotechnology* **2011**, *22*, 315301.
[19] J. Crangle, J. A. Shaw, *Philos. Mag.* **1962**, *7*, 207.
[20] Y. H. Huang, J. T. Wu, S. Y. Yang, *Microelectron. Eng.* **2011**, *88*, 849.
[21] K. L. Jim, F. K. Lee, J. Z. Xin, C. W. Leung, H. L. W. Chan, Y. Chen, *Microelectron. Eng.* **2010**, *87*, 959.
[22] K. Srinivasan, S. N. Piramanayagam, Y. S. Kay, *J. Appl. Phys.* **2010**, *107*, 033901-1.
[23] W. X. Xia, Y. Murakami, D. Shindo, M. Takahashi, *J. Appl. Phys.* **2009**, *105*, 013926-1.
[24] S. Hosaka, Z. Mohamad, M. Shirai, H. Sano, Y. Yin, A. Miyachi, H. Sone, *Microelectron. Eng.* **2008**, *85*, 774.
[25] M. Muechlberger, M. Boehm, I. Bergmair, M. Chouiki, R. Schoeftner, G. Kreindl, M. Kast, D. Treiblmayr, T. Glinsner, R. Miller, *Microelectron. Eng.* **2011**, *88*, 2070.
[26] Seagate. Press release: Seagate breaks areal density barrier: unveils the world's first hard drive featuring 1 terabyte per platerr. http://www.seagate.com/ww/v/index.jsp?vgnextoid=6fbdb5ebf32bf210VgnVCM1000001a48090aRCRD (May 2011).
[27] M. D. Austin, H. Ge, W. Wu, M. Li, Z. Yu, D. Wasserman, S. A. Lyon, S. Y. Chou, *Appl. Phys. Lett.* **2004**, *84*, 5299-1.
[28] M. D. Austin, W. Zhang, H. Ge, D. Wasserman, S. A. Lyon, S. Y. Chou, *Nanotechnology* **2005**, *16*, 1058.
[29] H. J. Richter, *Appl. Phys. Lett.* **2006**, *88*, 222512-1.
[30] K. R. Catchpole, A. Polman, *Opt. Express* **2008**, *16*, 21793.
[31] J. McPhillips, C. McClatchey, T. Kelly, A. Murphy, M. P. Jonsson, G. A. Wurtz, R. J. Winfield, R. J. Pollard, *J. Phys. Chem. C* **2011**, *115*, 15234.